

## The electrical switching phenomenon of a phase change memory using nitrogen doped $\text{Sb}_2\text{Te}_3$

Seung Yun Lee<sup>a</sup>, Sung Hyuk Cho<sup>a</sup>, Hyung Keun Kim<sup>a</sup>, Jin Ho Oh<sup>b</sup>, Hyeong Joon Kim<sup>b</sup>, Suk Kyoung Hong<sup>c</sup>,  
Jae Sung Roh<sup>c</sup> and Doo Jin Choi<sup>a,\*</sup>

<sup>a</sup>Department of Ceramic Engineering, Yonsei University, 134 Shinchon-dong, Sudaemun-ku, Seoul 120-749, Korea

<sup>b</sup>School of Material Science and Engineering, Inter-university Semiconductor Research Center, Seoul National University, Seoul 151-744, Korea

<sup>c</sup>Memory R&D Division, Hynix semiconductor Inc. San 136-1, Amiri, Bubal-eup, Ichon-si, Kyounggi-do 467-701, Korea

In order to increase the sheet resistance of  $\text{Sb}_2\text{Te}_3$  (ST) thin films, nitrogen-doped  $\text{Sb}_2\text{Te}_3$  (N-doped ST) thin films were deposited using DC magnetron sputtering. The nitrogen gas flow rate was changed from 0 sccm (ST(0)) to 6 sccm (ST(6)) during the deposition. The sheet resistances of N-doped ST films rapidly increased as the nitrogen gas flow rate increased. Phase-change random access memory (PRAM) test cells were fabricated using N-doped ST thin films. The threshold voltages of ST(0) and ST(6) PRAM test cells were 1.09 and 0.70 V, respectively. The mismatch problem of 1<sup>st</sup> and 2<sup>nd</sup> sweeping was hypothesized to be caused by poor adhesion and Te segregation between the ST film and TiN.

**Key words:**  $\text{Sb}_2\text{Te}_3$ (ST), PRAM, Threshold voltage, Nitrogen, Adhesion.

### Introduction

In recent years, the phase-change random access memory (PRAM) has been one of the most optimized candidates for the next generation non-volatile memory due to its fast operation speed, high scalability, low power operation and low fabrication cost [1]. For a PRAM to be a feasible candidate for a next generation memory, however, the reset operation power and duration of the set operation need to be reduced [2].  $\text{Ge}_2\text{Sb}_2\text{Te}_5$  (GST) has been widely studied and optimized as a PRAM material as its amorphous and crystalline phase transition is reversible and rapid. However, GST has several disadvantages including a relatively long crystallization time and a low resistance of the crystalline state for future PRAM applications [3, 4]. To address these problems, various investigations on new materials such as  $\text{Sb}_2\text{Te}_3$ (ST) [3],  $\text{Se}_x\text{Sb}_{100-x}$  [4] and  $\text{In}_x\text{Sb}_{100-x}$  [5] have been conducted. Of these materials, ST appears the most promising as it has been extensively optimized. In contrast to nucleation-dominated GST, the crystallization mechanism of ST is growth-dominated and the set operation time is shorter. In addition, the reset operation power of ST is lower than GST due to its relatively lower melting temperature [3]. However, since ST has a very low crystallization temperature, the data retention time is not guaranteed for PRAM applications though this drawback can be resolved by using dopants,

such as silver [6] and nitrogen [7]. To understand the effect of nitrogen doping on ST film, the sheet resistance of N-doped ST thin films and the electrical switching phenomenon of PRAM test cells using N-doped ST were investigated.

### Experiment

100 nm thick, N-doped ST thin films were deposited on a glass substrate by a DC magnetron sputtering system using a  $\text{Sb}_2\text{Te}_3$  (99.99%) composite target with various nitrogen gas flow rates at room temperature. During deposition, the total gas flow rate was fixed at 40 sccm and the ratio of Ar (99.999%) and  $\text{N}_2$  (99.9999%) gas flow was changed. The  $\text{N}_2$  gas flow rate was changed from 0 to 6 sccm to control the nitrogen content of N-doped ST thin films and these are designated ST(0) and ST(6) layers, respectively. The as-deposited ST(0) thin film had a crystalline structure showing a near metallic nature whereas as-deposited N-doped ST thin films were amorphous [7]. After deposition, the films were annealed at a temperature from 25 °C to 340 °C for 20 minutes under a high vacuum ( $3.0 \times 10^{-6}$  torr, 399.9  $\mu\text{Pa}$ ) chamber. The heating rate was 10  $\text{Kminute}^{-1}$ . The sheet resistance of the annealed films was measured by a four-point probe (CMT-SR2000N, Changmin Tech Co.). Since the ST(6) thin film showed the best effect of N-doping on sheet resistance, ST(0) and ST(6) were applied in PRAM test cells to confirm the N-doping effect on PRAM application. Fig. 1(a) shows a schematic cross sectional view of a PRAM test cell and Fig. 1(b) shows the top view of a PRAM test cell observed by a field-

\*Corresponding author:  
Tel : +82-2-2123-2852  
Fax: +82-2-365-5882  
E-mail: drchoidj@yonsei.ac.kr

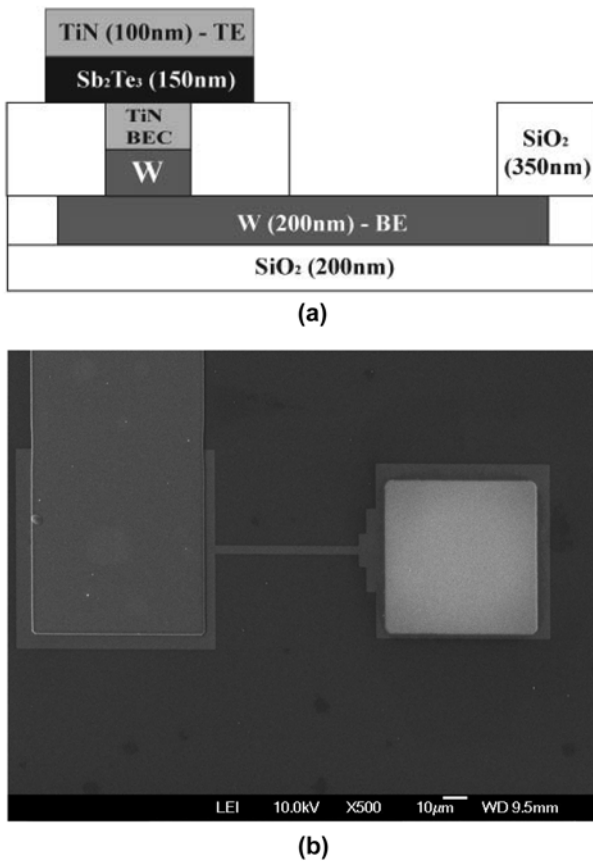


**Fig. 1.** (a) Schematic diagram of a cross sectional view of a PRAM test cell with a contact size of  $0.25\ \mu\text{m}$  and (b) top view of a PRAM test cell observed by FE-SEM.

emission scanning electron microscope (FE-SEM). The thickness of the ST layer was fixed at 150 nm and the diameter of the bottom electrode contact (BEC) was  $0.25\ \mu\text{m}$ . The electrical switching characteristic of the PRAM test cell was measured using a semiconductor parameter analyzer (HP-4155A, Hewlett-Packard). The applied currents ranged from 0 to 3 mA and the corresponding voltage was measured simultaneously. To confirm the adhesion between ST and TiN, 200 nm ST(0) and ST(6) thin films were deposited on 100 nm TiN/100 nm SiO<sub>2</sub>/Si. A scratch test was performed using a CSEM Revetest Scratch-Tester. The loading speed and scratch speed of the tester were  $50\ \text{N}\ \text{minute}^{-1}$  and  $3\ \text{mm}\ \text{minute}^{-1}$ , respectively. The minimum load of the scratch tester was 2 N.

## Results and Discussion

The sheet resistance changes of N-doped ST thin films are shown in Fig. 2. The sheet resistance of as-deposited ST(0) was approximately  $1 \times 10^5\ \Omega/\square$ . In contrast, the as-deposited N-doped ST films showed very high sheet resistance (over  $5 \times 10^6\ \Omega/\square$ ) which was nearly two orders of magnitude greater than that of ST(0) since N-doped ST films were amorphous. Since N-doping in the ST film probably decreased the grain size and increased the

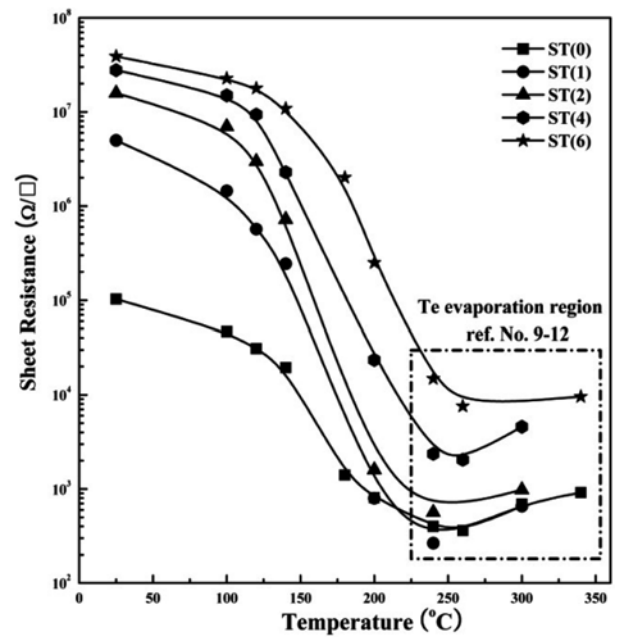


**Fig. 2.** The sheet resistance of N-doped ST thin films with nitrogen gas flow between 0 and 6 sccm.

grain boundary by suppressing grain growth, similar to GST, the sheet resistance of N-doped ST thin films were greater than that of ST(0) [7, 8]. At all of the annealing temperatures, the N-doped ST film showed greater sheet resistance than the ST(0) film, except for ST(1). The amount of nitrogen in ST(1) was too small to increase the sheet resistance of the crystalline state. Moreover, the sheet resistances of ST(0), ST(1) and ST(2) dramatically decreased above  $100\ ^\circ\text{C}$ , and ST(4) and ST(6) decreased at  $120\ ^\circ\text{C}$  and  $140\ ^\circ\text{C}$ , respectively. This rapid drop was caused by crystallization to a rhombohedral structure. Since N-doping increased the crystallization temperature of ST thin films by suppressing grain growth, the thermal stability of N-doped ST thin films was greater than that of ST(0) [7]. All of the N-doped ST thin films showed an increase in the sheet resistance when the annealing temperature was greater than  $240\ ^\circ\text{C}$ . The increase in sheet resistance was probably caused by evaporation of Te due to the lower melting temperature ( $449.57\ ^\circ\text{C}$ ) and high vapor pressure of Te [9-12]. Hence, the N-doping of ST films increased the sheet resistance and thermal stability of ST thin films [7].

The electrical switching phenomena of fabricated (a) ST(0) and (b) ST(6) PRAM test cell are shown in Fig. 3. Since the resistance of the test cell was very high at the beginning of the test in which the phase was amorphous, the current in the cells was nearly negligible. However, the current value suddenly increased at a threshold voltage ( $V_{\text{th}}$ ) showing voltage snap-back, which is a typical phenomenon of chalcogenides. At a certain threshold voltage above the set operation voltage, the Joule heating was high enough to allow spontaneous crystallization to the low resistance crystalline state [13]. The threshold

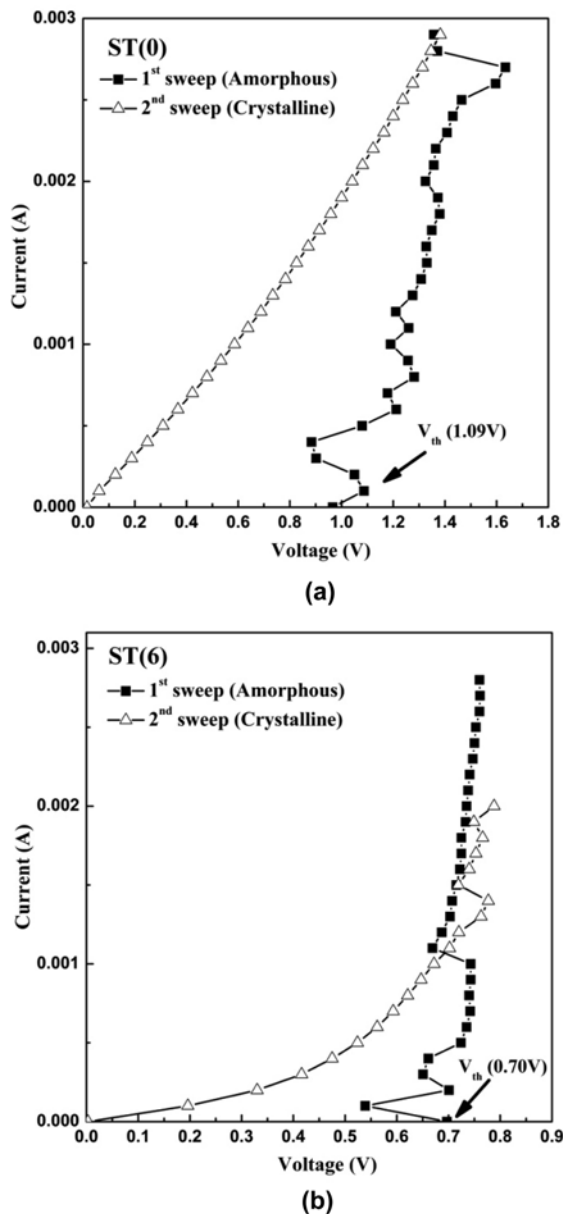


**Fig. 3.** The I-V characteristics of the (a) ST(0) and (b) ST(6) PRAM test cells.

voltages of ST(0) and ST(6) were 1.09 and 0.70 V, respectively. The threshold voltage of ST(6) was less than that of the ST(0). This threshold voltage reduction of ST(6) was hypothesized to be correlated to the difference of sheet resistance between ST(0) and ST(6). According to Fig. 2, as the N-doping increased the sheet resistance, the Joule heating of ST(6) became far more efficient than that of ST(0). Hence, the threshold voltage of ST(6) was much lower than that of ST(0).

The switching behaviors of fabricated ST(0) and ST(6) PRAM test cells showed a mismatch problem between the 1<sup>st</sup> and 2<sup>nd</sup> sweeping, as shown in Fig. 3. One reason for this phenomenon may be an adhesion problem [5] between the ST and TiN during the 1<sup>st</sup> and 2<sup>nd</sup> sweeps. Scratch tests were therefore performed to

investigate the adhesion between ST and TiN. Critical loads of all of the ST thin films were less than 2 N, except the amorphous ST(0) which was approximately 2.2 N. Therefore, the adhesion between ST and TiN was very poor. During the switching process, ST thin films experience large amounts of thermal energy to change their phase which induces a volume change. In turn, this volume change is converted into large amounts of thermal stress. As ST and TiN had poor adhesion, the interface may be delaminated by the thermal stress [5]. In the case of GST (100 nm) on  $SiO_2/Si$  (730  $\mu m$ ), the thermal stress was so great (approximately 100 MPa) that the GST could have plastically deformed in the film [14]. Another cause of the mismatch problem may be segregation of Te between ST and TiN. In the case of the TiN/GST/ $SiO_2$  multilayer, the Te in the GST easily diffuses to the TiN and GST interface due to its low melting temperature and relatively high mobility. When Te segregates at the interface, it begins grain growth and introduces tiny voids at temperatures greater than 200 °C. The voids and Te deficiency reduce the PRAM cycling time in the GST [11, 12]. The Te in the ST thin films may have segregated and produced voids between ST and TiN, similar to the case of GST. Hence, the poor adhesion between ST and TiN was much worse during the sweepings. Although N-doped ST has poor adhesion and Te segregation at the interface, N-doped ST has a very short crystallization time and a high resistance crystalline state. These characteristics make N-doped ST one of the most optimized materials for PRAM applications.

## Conclusions

The electric switching phenomenon of ST(0) and ST(6) PRAM test cells were investigated to understand the effect of nitrogen doping on ST. Since N-doping increased the sheet resistance of ST thin films, the threshold voltage of ST(6) was relatively lower than that of ST(0). This indicates that N-doping of ST may decrease energy consumption during its application in a PRAM. However, 1<sup>st</sup> and 2<sup>nd</sup> sweepings showed a mismatch problem, which may be due to poor adhesion and Te segregation between the ST and TiN. A solution may be to use a very thin adhesive buffer layer between ST and TiN to reduce the thermal expansion mismatch [15].

## Acknowledgement

This work was supported by the Second Stage of Brain Korea 21 project in 2007 and Hynix Semiconductor Inc. of Korea.

## References

1. M.H.R. Lankhorst, B.W.S. M.M. Ketelaars, and R.A.M. Wolters, *Nat. Mater.* 4 (2005) 347-352.
2. S. Lai, *IEDM Tech. Dig.* (2003) 255-258.
3. B. Liu, Z. Song, S. Feng, and B. Chen, *Microelectron.*

- Eng. 82 (2005) 168-174.
4. M.J. Kang, S.Y. Choi, D. Wamwangi, K. Wang, C. Steimer, and M. Wuttig, *J. Appl. Phys.* 98 (2005) 014904-1~14904-6.
  5. H.O. Lee, D.H. Kang, *Jpn. J. Appl. Phys.* 44[7A] (2005) 4759-4763.
  6. J. Xu, B. Liu, Z. Song, S. Feng, and B. Chen, *Mater. Science and engineering B* 127 (2006) 228-232.
  7. M.S. Kim, S.H. Cho, S.K. Hong, J.S. Roh, and D.J. Choi, *Ceram. Int.* 34 (2008) 1043-1046.
  8. S.M. Kim, J.H. Jun, D.J. Choi, S.K. Hong, and Y.J. Park, *Jpn. J. Appl. Phys.* 44[6] (2005) L208-L210.
  9. H. Lv, P. Zhou, Y. Lin, T. Tang, B. Qiao, Y. Lai, J. Feng, B. Cai, and B. Chen, *Microelectron J.* 37 (2006) 982-984.
  10. G. Ghosh, *J. Phase Equilibria* 15[3] (1994) 349-360.
  11. L. Krusin-Elbaum, C. Cabral, Jr., K.N. Chen, M. Copel, D.W. Abraham, K.B. Reuter, S.M. Rossnagel, J. Bruley, and V. R. Deline, *Appl. Phys. Lett.* 90 (2007) 141902-1~141902-3.
  12. C. Cabral, Jr., K.N. Chen, L. Krusin-Elbaum, and V. Deline, *Appl. Phys. Lett.* 90 (2007) 051908-1~051908-3.
  13. A. Pirovano, A.L. Lacaita, A. Benvenuti, F. Pellizzer, and R. Bez, *IEEE Trans. Electron Devices* 51[3] (2004) 452-459.
  14. K.N. Chen, L. Krusin-Elbaum, C. Cabral, Jr., C. Lavoie, J. Sun, and S. Rossnagel, 21<sup>st</sup> IEEE NonVol. Semi. Mem. Workshop (2006) 97-98.
  15. A. Ebina, M. Hirasaka, J. Isemoto, A. Takase, G. Fujinawa, and I. Sugiyama, *Jpn. J. Appl. Phys.* 40[3B] (2001) 1569-1574.